Phase Transitions in Concentrated DNA Solutions: Ionic Strength Dependence

Teresa E. Strzelecka*,† and Randolph L. Rill

Institute of Molecular Biophysics and Department of Chemistry, Florida State University, Tallahassee, Florida 32306

Received January 16, 1991; Revised Manuscript Received April 8, 1991

ABSTRACT: Anisotropic-phase formation in concentrated solutions of short (~500 Å) DNA fragments with excess Na^+ concentrations of 0.01, 0.1 and 1.0 M was investigated by phosphorus-31 NMR spectroscopy and optical microscopy. The phase diagrams for isotropic- to liquid-crystalline-phase transitions were determined for each Na^+ concentration and were found to be in good qualitative agreement with theoretical predictions. The critical DNA concentration required for the anisotropic-phase formation was found to be weakly dependent on the excess Na^+ concentration. The effective DNA radii, estimated by comparing the experimental phase boundaries with theoretical ones are in very good agreement with other experimental and theoretical values. They depend on the *effective* Na^+ concentration in solution, defined as the excess Na^+ concentration +24% of the DNA phosphate concentration. The anisotropic phases formed at all Na^+ concentrations and their succession with increasing DNA concentration in solution are described.

Introduction

Understanding of DNA packaging in living organisms requires the knowledge of DNA–counterion and DNA–DNA interactions in condensed state. Therefore, physicochemical studies of concentrated DNA solutions not only advance the field of physical chemistry of charged polymers, but also provide insights into the biologically important process of DNA packaging. DNA concentrations in phage heads and nuclei of eucaryotic cells are of the order of hundreds of milligrams per milliliter of volume. In several cases this "high-density" state corresponds to a spatially ordered arrangement of DNA molecules, usually referred to as a "liquid-crystalline state". Sipski and Wagner[1] showed that a large, negative ellipticity observed in the CD spectra of chromosomal preparations from equine sperm cells can be explained if a cholesteric arrangement of DNA molecules in the chromosomes is assumed. Liquid-crystalline organization of DNA molecules was also proposed for dinoflagellate (*Prorocentrum micans*) chromosomes on the basis of microscopic studies.[2-5] Hexagonal packing was proposed for DNA molecules in the heads of phages T7,[5] T2 and λ,[6] P22,[8] and *φ29*.[9]

In vitro short DNA molecules behave like rigid rods in aqueous solutions. Therefore, according to theoretical predictions of Onsager[10] and Flory,[11,12] DNA solutions should separate into the isotropic and anisotropic phases when the DNA concentration exceeds a critical value. In fact, liquid-crystalline phases of DNA have been studied extensively since they were first observed by Robinson.[13] In the majority of cases the anisotropic phase observed was cholesteric,[4,14-20] but a weakly birefringent, precholesteric phase,[21,22] and more highly ordered phases,[22-24] have been reported. The anisotropic phase can also be formed in rather dilute DNA solutions after addition of a strongly hydrophilic polymer.[25,26] This phenomenon was called "ψ condensation", which is an abbreviation for "polymer- and salt-induced condensation". Hexagonal packing of DNA helices, with interhelical spacings similar to that found in phage heads, was found in DNA crystals grown from water–ethanol mixtures.[27,28]

Despite a large amount of experimental data the mechanism of DNA condensation at the molecular level is far from clear; therefore, we have undertaken a comprehensive study of the phase transition behavior in concentrated solutions of short (~500 Å) DNA fragments. Phase diagrams were constructed for isotropic to liquid-crystalline transitions in concentrated DNA solutions at three supporting electrolyte concentrations (0.01, 0.1, and 1.0 M Na^+) and a temperature range of 20–60 °C, and ^{23}Na NMR studies of counterion behavior in these solutions were performed. The sodium NMR data will be presented in a separate paper (in preparation). We hope that our results will also help in the development of more accurate theories of DNA–counterion and DNA–DNA interactions in aqueous solutions.

Experimental Section

DNA Isolation and Sample Preparation. DNA fragments of 147 base pairs (bp) were isolated from nucleosome core particles as described previously.[17] A set of DNA solutions with concentrations ranging from 10 to 300 mg of DNA/mL of solvent was prepared in a way that permitted control of the total and excess Na^+ concentrations.

Essentially salt free DNA was obtained by prolonged dialysis against 0.5 mM Na^+ buffer, performed under vacuum from a water aspirator in a collodion bag device (Schleicher and Schull) to minimize dilution. The total Na concentration of the DNA solutions after dialysis was determined by nuclear activation analysis of diluted aliquots, performed in the University of Florida Training Reactor Facility in Gainsville. The DNA phosphate concentration was determined from the absorbance at 260 nm, using the extinction coefficient of 6600 M^{-1} cm^{-1}.

DNA samples in 0.01 M Na^+ buffer were prepared from a dialyzed DNA solution with 0.127 (±0.004) M phosphate and 0.129 (±0.003) M Na^+. The DNA solutions from which 0.1 M Na^+ samples were prepared had a phosphate concentration of 0.121 (±0.004) M and a Na^+ concentration of 0.121 (±0.003) M. DNA samples in 1.0 M Na^+ buffer were prepared from DNA solutions with a phosphate concentration of 0.124 (±0.003) M and a Na^+ concentration of 0.124 (±0.002) M. Aliquots of DNA solutions containing total DNA masses of 5, 10, ..., 150 mg were transferred to microfuge tubes and dried under vacuum in a Speed-Vac centrifugal concentrator (Savant Instruments, Inc.), and then 500 mL of Na^+ buffer (0.01, 0.1, or 1.0 M) was added to each tube, giving a set of 30 DNA samples with concentrations of 10, 20, ..., 300 mg of DNA/mL of solvent and an excess Na^+ concentration of 0.01, 0.1, or 1.0 M. Errors in the DNA concentrations are estimated to be less than 3%. The above concentrations are related to the more commonly used concentrations of milligram of DNA per milliliter of solution by *C* (mg

† Current address: Department of Biochemistry and Molecular Biophysics, College of Physicians and Surgeons, Columbia University, New York, New York 10032.

0024-9297/91/2224-5124$02.50/0 © 1991 American Chemical Society

of DNA/mL of solution) = C' (mg of DNA/mL of solvent)[$V/(g_D v_D + V)$], where V is the solvent volume, g_D is the DNA mass, and v_D is the partial specific volume of DNA, equal to 0.55 cm^3/g. Unless stated otherwise, the DNA concentrations used throughout this paper are expressed in conventional units of milligrams of DNA per milliliter of solution.

Phosphorus-31 NMR Spectroscopy. Phosphorus-31 NMR spectra were taken for nonspinning samples at a phosphorus frequency of 61.28 MHz by use of a multinuclear spectrometer equipped with wide-bore superconducting solenoid and quadrature detection. Gated proton decoupling was used during the data acquisition. Spectra were taken with a sweep width of ±5000 Hz and a pulse repetition time of 12.5 s (the phosphorus T_1 was 2.45–2.50 s for all ionic strengths and DNA concentrations); 100 scans were collected for each spectrum.

DNA samples were placed in 1.5-mL cylindrical tubes, cut in such a way that 500 μL of solution filled them without creating air bubbles. Since the anisotropic phases have higher density than the isotropic phase, they tend to settle at the bottom of NMR tubes; therefore, we have used a specially constructed NMR probe, in which all of the sample tube could be placed horizontally within the receiver coil.

Temperature was controlled by a thermocouple to within ±1 °C. Each sample was equilibrated for 1 h at 20 °C in the magnet before the first spectrum was taken. Spectra at higher temperatures (30–60 °C) were taken at least 30 min after the temperature change. Resonance areas were obtained with a line-deconvolution program on the Nicolet-1180 computer. The relative error of resonance area determination was usually lower than 1%, and the error of fitting procedure was of the order of 1–2%.

The equilibration times of DNA solutions during the temperature changes were determined experimentally. During the test run the sample was placed in the magnet at 20 °C and spectra were taken every 10 min. The time after which the areas of isotropic and anisotropic resonances no longer changed (within experimental error) was taken as an equilibration time. At 20 °C it was found to be 30 min. The same procedure was used to determine equilibration times at higher temperatures, and these times at 30–60 °C were found to be 10–15 min. A few experiments on the same set of samples, performed 2 months after the first experiments, gave identical resonance areas. Furthermore, microscopic examination showed that phase changes occurred rapidly and reversibly with temperature changes, yielding stable textures within minutes after perturbation.[29,30] Sample textures were stable for prolonged periods in the absence of drying.

Phase Diagram Construction from the ^{31}P NMR Data. Solid-state ^{31}P NMR spectra of DNA solutions can be used to determine the phase diagram boundaries for isotropic to liquid-crystalline transitions, which take place in concentrated DNA solutions.[17] When the DNA solution is isotropic, only a single Lorentzian resonance is observed, and its line width increases slowly with increasing DNA concentration as the anisotropic-phase boundary is approached.[17,29,30] In biphasic solutions, where the isotropic and anisotropic phases coexist, the ^{31}P spectrum is a superposition of two resonances: a relatively sharp resonance, corresponding to the isotropic phase, and a broad resonance of the anisotropic phase. The line shapes of anisotropic-phase resonances were always Gaussian. The phase state of each sample used for NMR experiments was verified by polarized light microscopy.

Phase diagrams for isotropic- to liquid-crystalline-phase transitions in polymer solutions are usually presented in terms of the polymer volume fraction vs temperature. The determination of DNA volume fraction from the DNA concentration requires knowledge of the effective DNA radii, which were not known for concentrated DNA solutions. Theoretical estimates of the effective DNA radii at various ionic strengths exist only for dilute DNA solutions and therefore cannot be directly applied to concentrated solutions. Brian et al.[31] showed that the effective DNA radii calculated from Poisson–Boltzmann theory are consistent with the nonideal behavior of moderately concentrated DNA solutions at ionic strengths above 0.1 M NaCl. It is not certain, however, that these radii can be used for highly concentrated DNA solutions, where DNA molecules are forced to lie very close to each other. The procedure adopted by us was to construct the phase diagram (at a given excess Na^+ concentration) in terms of DNA concentration vs temperature and then, by comparison with theoretically predicted phase diagrams, estimate the effective DNA radius and volume fraction. A detailed description of phase diagram construction was published earlier;[29,30] therefore it will not be repeated here.

Microscopy. Samples of DNA solutions were placed on a glass slide (cleaned by soaking in concentrated nitric acid), covered with a cover slip, sealed with Permount (Fisher Scientific), and then observed through crossed polarizers with a Nikon Optiphot-Pol microscope under 3200 K tungsten–halide illumination.

Results

Polarized Light Microscopy. The microscopic textures of different DNA samples were described in detail previously;[17,29] therefore only a short summary will be given here.

(1) DNA Solutions in 0.01 M Na^+ Buffer. DNA samples with concentrations from 147 to 172 mg/mL were quite viscous and transparent. When viewed between crossed polarizers, the weakly birefringent areas, coexisting with small spherulites, could be seen. Viewed at a higher magnification, these weakly birefringent areas revealed the presence of the inversion walls characteristic of a nematic mesophase. The sign of birefringence in these samples was positive, also pointing to a nematic ordering of DNA molecules.

As the DNA concentration increased, small islands of cholesteric order, growing from the weakly birefringent areas, appeared and increased in size with an increasing amount of DNA in solution. When the DNA concentration reached 188 mg/mL, samples showed textures characteristic of a cholesteric phase, coexisting with the areas of isotropic and weakly birefringent phases. With DNA concentration reaching 204 mg/mL there was still a small amount of isotropic phase present in the sample, but the appearance of a third anisotropic phase could be observed. Some of the textures of this phase resembled textures characteristic of nematic mesophase and others were similar to the textures observed in smectic samples.[32] Other textures exhibited by these samples showed cholesteric ordering.

The response to temperature changes were observed in the 180 and 250 mg/mL samples. In the first sample, melting of the cholesteric phase proceeded through the formation of small isotropic areas, which increased in size with increasing temperature. At the border between the cholesteric and isotropic phases there was a region of weakly birefringent phase. These changes were quite rapid. It took only about 1–3 min from the time of temperature increase for the sample to adopt a new texture, and the reversal to the anisotropic phase was just as rapid. A similar behavior was observed in the 250 mg/mL sample, but without the formation of a weakly birefringent phase with increasing temperature.

(2) DNA Solutions in 1.0 M Na^+ Buffer. The lowest DNA concentration at which the first trace of the anisotropic phase could be observed was 196 mg/mL, and the phase was weakly birefringent. As the DNA concentration increased, the cholesteric phase appeared in the form of small spherulites. At higher DNA concentrations the amount of cholesteric phase increased, and the 250 and 257 mg/mL samples were fully liquid crystalline, with textures indicating cholesteric ordering of DNA molecules. Temperature behavior of all the samples was very similar. The melting of cholesteric phase proceeded through the formation of small isotropic areas, which increased in size with increasing temperature.

(3) DNA Solutions in 0.1 M Na^+ Buffer. The microscopic textures observed in these solutions were similar to the textures of the 1 M Na^+ samples. The lowest DNA concentration at which the anisotropic phase appeared was 164 mg/mL. The temperature behavior of these samples was the same as in the 1 M Na^+ samples.

Phosphorus-31 NMR Data. ^{31}P NMR resonances observed in concentrated DNA solutions at all ionic strengths were either Lorentzian (for isotropic samples), Gaussian (for fully liquid crystalline samples), or a superposition of the two for the biphasic samples. The observed line widths did not exceed 14 ppm in any of the samples. This value is much smaller than the 200 ppm line width of the powder pattern of solid, B-form, hydrated DNA,[33-35] indicating that the motional dynamics of DNA molecules are not strongly affected by anisotropic-phase formation.

Interpretation of the observed NMR line widths in terms of molecular dynamics requires proof that the resonances are homogeneous, especially in the case of Gaussian lines, which, in nonhomogeneous systems, are envelopes of many Lorentzian lines. Two experiments were performed to determine whether the lines observed for our DNA solutions were homogeneously broadened. In the first experiment a narrow frequency band near the tail of a broad resonance was irradiated by a weak radiofrequency pulse, and the signal was collected after the 90° pulse. If the line is homogeneous, the total resonance intensity will decrease, whereas in the case of nonhomogeneous broadening, one of the lines at the frequency of a weak pulse will disappear, forming a "hole" in the resonance. The second experiment was a spin–echo experiment in which the values of the delay times between pulses were varied. For homogeneous resonance and delay time values longer than T_2 ($1/\Delta\nu_{1/2}$), the resonance will disappear, whereas if it is a collection of narrow lines, it will not. The results of both experiments for the 250 mg/mL sample (in 0.01 M Na^+ buffer) demonstrated that the lines were homogeneously broadened.[29]

If there were no other processes contributing to resonance broadening, the increasing line widths with increasing DNA concentration could be related to decreased mobility of DNA molecules in the anisotropic phase. For molecular motions with correlation times longer than 5×10^{-8} s, R_2 ($1/T_2$) is proportional to the correlation time;[36] therefore, since the slower molecular motion means longer correlation times, the resonance will broaden when molecules become less mobile. However, in the case of DNA solutions at all three ionic strengths, the line widths were also affected by the degree of magnetic alignment of DNA molecules. As reported previously,[17] the resonance line width increased when the solutions became biphasic and then narrowed when a fully liquid crystalline phase was found. Changes in the line width were paralleled by changes in the separation, δ, between the isotropic and anisotropic resonances and showed a complex behavior as a function of temperature and DNA concentration[29,30] (see also the next section). In general, narrowing of the resonances with increasing temperature was accompanied by an increase in their separation, indicating increased magnetic alignment of DNA molecules in the anisotropic phase. In conclusion, the observed changes in the ^{31}P NMR line widths cannot be interpreted simply in terms of either magnetic alignment or motional dynamics of DNA molecules.

The T_1 relaxation times determined for several samples in the range of 121–250 mg/mL (in 0.01 M Na^+) showed a decrease from 2.50 for the 121 mg/mL sample to 2.45 s for the 250 mg/mL sample. Since the longitudinal relaxation of phosphorus nuclei is dominated by fast, internal motions of the DNA backbone,[37,38] the fact that T_1 does not change (within limits of experimental error) when the solutions undergo transitions from the isotropic to fully liquid crystalline phase indicates that the backbone motions are not affected by the anisotropic-phase formation.

Phase Diagrams for Isotropic- to Liquid-Crystalline-Phase Transitions. The DNA concentrations at which the anisotropic phase appears (C_i) and at which the isotropic phase disappears (C_a) were determined from the plots of Cf_a vs C (where f_a is the fraction of DNA molecules in the anisotropic phase and C the total DNA concentration in solution) according to eq 10[30] from the NMR data for the three Na^+ concentrations. The construction of the phase diagram for 0.01 M Na^+ (Figure 1A) was described earlier.[30] Figure 1B shows the phase diagram for isotropic to liquid-crystalline transitions in 0.1 M Na^+ buffer, determined from the NMR data obtained from samples with DNA concentrations of 164–257 mg/mL, and Figure 1C presents the phase diagram for 1.0 M Na^+ buffer, calculated from data for the DNA concentration range of 220–257 mg/mL. The three phase diagrams are superimposed in Figure 1D.

The plots of Cf_a vs C used to construct these phase diagrams are shown in Figure 2 for 0.1 M Na^+ buffer (A) and 1.0 M Na^+ buffer (B). The lines at 20, 30, 50, and 60 °C (0.1 M Na^+) and at 20, 30, and 40 °C (1.0 M Na^+) were originally fit with one straight line, but the two-line fit shown here proved to be more accurate (on the basis of higher correlation factors). A similar fitting procedure was performed for the 0.01 M Na^+ data, and the DNA concentrations, corresponding to the intersections of two straight-line segments for a given temperature, correlated well with microscopic data, indicating the appearance in solution of a third anisotropic phase. However, in both 0.1 and 1.0 M Na^+ samples we observed only two anisotropic phases: a precholesteric, weakly birefringent phase and a cholesteric phase. Therefore, these inflection points might indicate DNA concentrations where the precholesteric phase totally disappears. Indeed, microscopic observation proved that for DNA concentrations exceeding 220 mg/mL in 0.1 M Na^+ buffer and 235 mg/mL in 1.0 M Na^+ buffer only the isotropic and cholesteric phases coexisted in solution. In the case of 0.1 M Na^+ samples, the inflection points of the 20, 30, 50, and 60 °C Cf_a vs C curves correspond to the regions on the δ vs C plots (Figure 3A), where δ (the separation between isotropic and anisotropic resonances) has reached a constant value. However, for the 1.0 M Na^+ samples, the δ vs C curves do not show any obvious plateau at ~235 mg/mL (20 and 30 °C, Figure 3B).

The most obvious difference between the three phase diagrams presented in Figure 1 is the relative simplicity of the phase diagrams for the 0.1 and 1.0 M Na^+ buffers. Regions II and III in Figure 1A are triphasic, whereas in parts B and C of Figure 1 only region II is truly triphasic, with the isotropic, precholesteric, and cholesteric phases in coexistence. The total width of the region separating the fully isotropic (I) and fully liquid crystalline phase (IV) is ~125 mg/mL for 0.01 M Na^+, ~135 mg/mL for 0.1 M Na^+, and ~100 mg/mL for 1.0 M Na^+ buffer (at 20 °C). The boundary separating the fully isotropic region I from the triphasic region II (we shall call it the isotropic boundary) is almost identical (within experimental error) for the 0.01 and 0.1 M Na^+ buffers and is shifted toward higher DNA concentrations in 1.0 M Na^+ buffer (Table

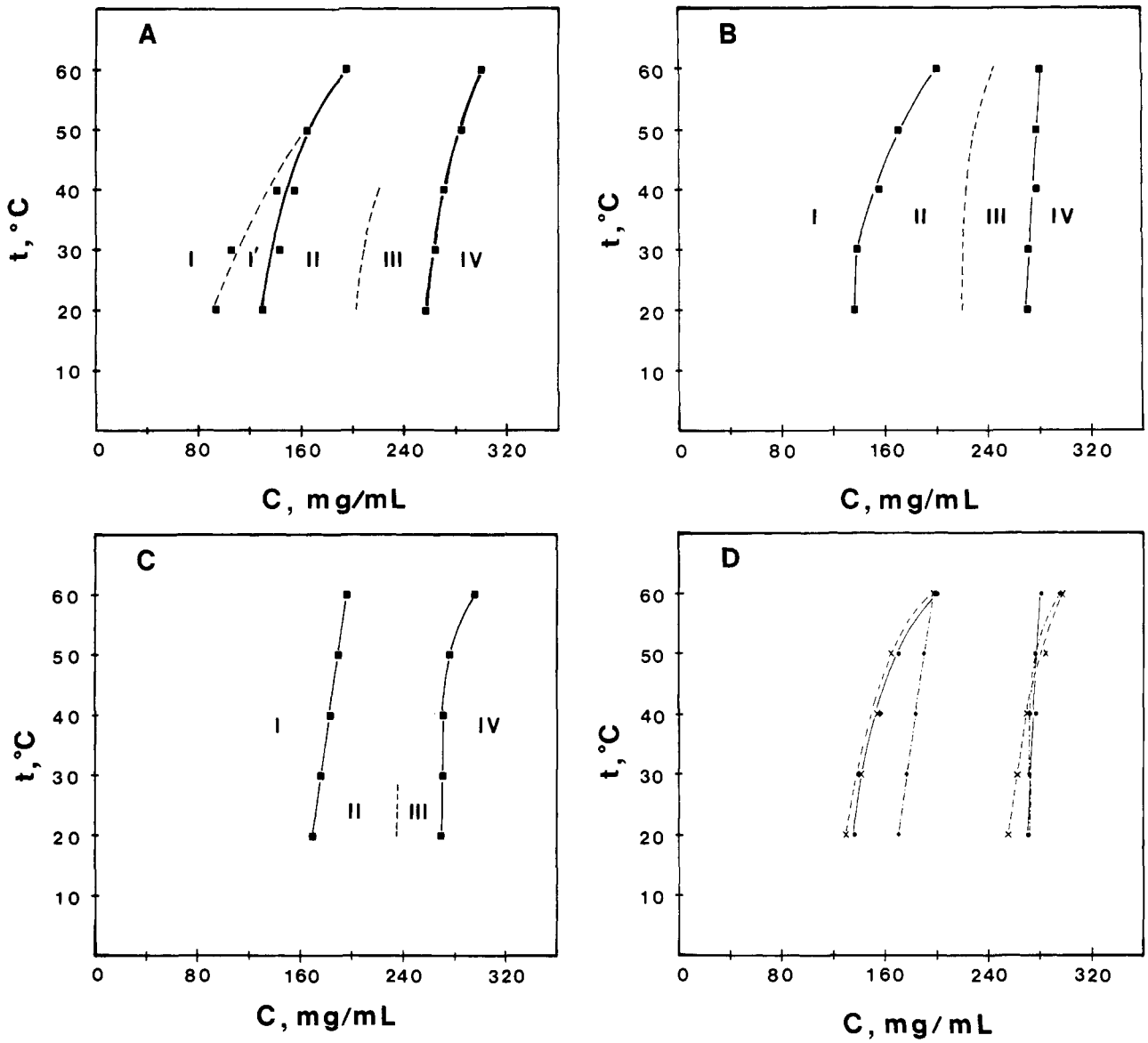

Figure 1. Phase diagrams for isotropic- to liquid-crystalline-phase transitions in concentrated DNA solutions at three excess Na^+ concentrations. (A) 0.01 M Na^+ buffer: region I is isotropic; region I' is isotropic but exhibits higher viscosity and broader ^{31}P resonances than region I; region II is triphasic (isotropic + precholesteric + cholesteric); region III is also triphasic (isotropic + cholesteric + higher order phase); region IV is fully anisotropic (cholesteric + higher order phase). (B) 0.1 M Na^+ buffer: region I is isotropic; region II is triphasic (isotropic + precholesteric + cholesteric); region III is biphasic (isotropic + cholesteric); region IV is fully cholesteric. (C) 1.0 M Na^+ buffer: region I is isotropic; region II is triphasic (isotropic + precholesteric + cholesteric); region III is biphasic (isotropic + cholesteric); region IV is fully cholesteric. The dashed lines indicate the DNA concentrations that correspond to the inflection points in parts B and C of Figure 2 (see Results). (D) Superposition of the three phase diagrams: (– –×– –) 0.01, (–·–) 0.1, (– · ● · –) 1.0 M Na^+ buffer.

I, Figure 1D). However, it should be noted that the effective Na^+ concentrations (defined as the excess Na^+ concentration +24% of the DNA phosphate concentration) at this boundary (at 20 °C) are 0.11 M in 0.01 M Na^+ buffer and 0.2 M in 0.1 M Na^+ buffer. Therefore, one expects to see very little difference in the DNA concentrations of these two isotropic boundaries. In the case of 1.0 M Na^+ buffer the isotropic boundary is at higher DNA concentrations, since at the effective Na^+ concentration of ~1.1 M the DNA helices have smaller effective radii and are better electrostatically screened from each other. On the other hand, the boundary separating regions III and IV (the anisotropic boundary) has very similar DNA concentration and temperature dependence for the 0.1 and 1.0 M Na^+ buffers, but is more temperature dependent for the 0.01 M Na^+ buffer (Figure 1D). This can be due to the fact that in the case of the two higher Na^+ concentrations region IV consists of only one phase (cholesteric), whereas in 0.01 M Na^+ region IV is a mixture of a cholesteric and a higher order phase.

Comparison with Theories of Liquid-Crystalline-Phase Formation. The phase diagrams for isotropic- to liquid-crystalline-phase transitions are presented here in terms of DNA concentration vs temperature, instead of DNA volume fraction vs temperature, as is customary for polymer solutions. Since we do not know the effective DNA radii in concentrated solutions, we can only estimate them by comparing our data with theoretically predicted phase diagrams. Onsager[10] proposed that charged polymer molecules should be treated as if they had an effective diameter determined by the extent of the electric double layer surrounding them. In practical terms, the extent of the double layer is determined by the smallest distance at which two DNA helices can approach each other. We have estimated the effective radii of DNA molecules in our solutions by comparing the experimental phase

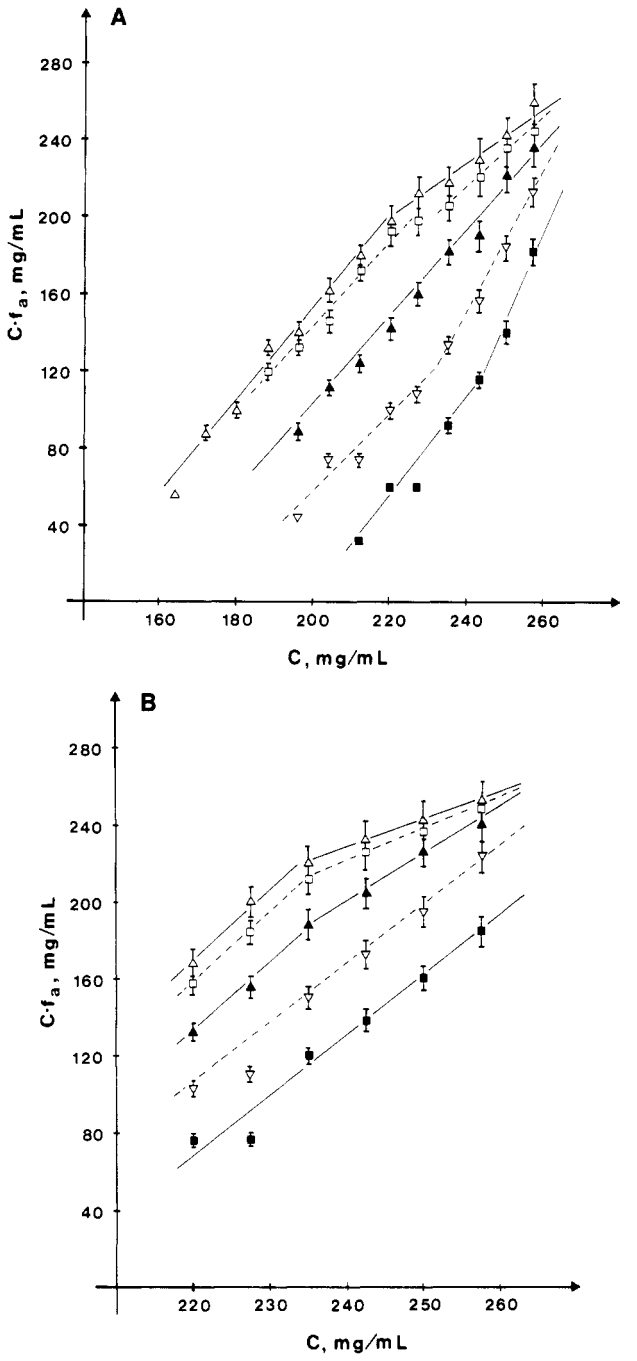

Figure 2. Plots of Cf_a vs C for 0.1 (A) and 1.0 M (B) Na^+ buffer. (△) 20, (□) 30, (▲) 40, (▽) 50, and (■) 60 °C.

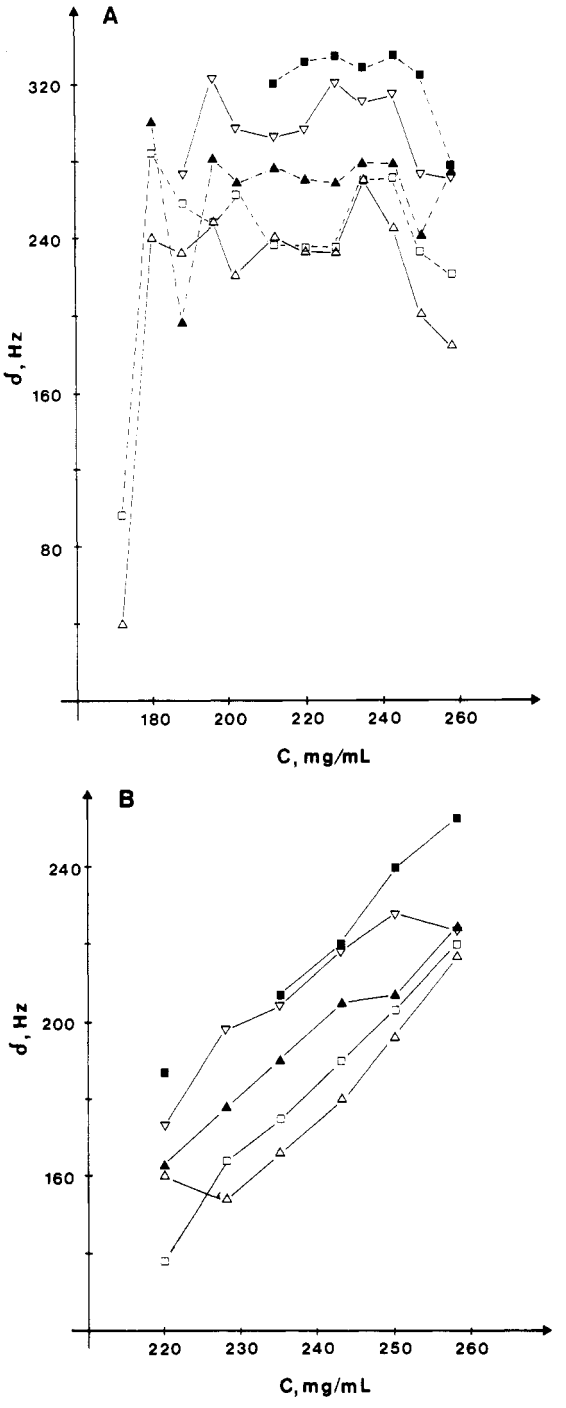

Figure 3. Dependence of δ (the separation between the isotropic and anisotropic ^{31}P NMR resonances) on DNA concentration and temperature for 0.1 (A) and 1.0 M (B) Na^+ buffer. (△) 20, (□) 30, (▲) 40, (▽) 50, and (■) 60 °C.

diagram boundaries with the theory of Flory[11,1]12 and by calculating theoretical phase diagrams according to Stroobants et al.[39]

Fit to Flory's Theory. This theory, based on lattice statistics, treats polymer molecules as hard rods, with interactions between rod segments described (in the most recent version) in terms of the Mayer–Saupe potential.[40-42] The critical polymer concentration required for the formation of an anisotropic phase is predicted to be strongly dependent on the polymer axial ratio and only weakly dependent on temperature. The predicted phase diagram has a narrow biphasic region between the isotropic and anisotropic phases. Since the phase transitions described here and previously[16,17] are qualitatively consistent with the predictions of Flory's theory, we have fit the concentrations at the isotropic (C_i) an anisotropic (C_a) boundaries to Flory's theory.[12] This fit assumes that the charged DNA molecules can be replaced by rods with effective radii that include the counterion atmosphere. The details of the fitting procedure were described earlier,[17,30] and the results are shown in Table II for all three ionic strengths at 20, 40, and 60 °C.

Not surprisingly, the best-fit effective radii of DNA molecules in 0.01 and 0.1 M Na^+ buffer were virtually identical for both the isotropic and anisotropic boundaries. The effective DNA radii in 1.0 M Na^+ buffer are lower by ~4 Å at 20 °C at the isotropic boundary, but this difference disappears at 60 °C. Also, the effective DNA radii at the anisotropic boundary are almost the same for all three Na concentrations and temperatures. The effective DNA radius is moderately dependent on temperature in the 0.01 and 0.1 M Na^+ buffers, but only slightly in the 1.0 M

Table I
Dependence of the Isotropic- (C_i) and Anisotropic- (C_a) Phase Boundaries on Temperature and Na^+ Concentration[a]

	0.01 M Na^+		0.1 M Na^+		1.0 M Na^+	
t, °C	C_i, mg/mL	C_a, mg/mL	C_i, mg/mL	C_a, mg/mL	C_i, mg/mL	C_a, mg/mL
20	131 (0.10)	256 (0.20)	136 (0.20)	271 (0.30)	171 (1.12)	270 (1.20)
30	142 (0.11)	263 (0.20)	137 (0.20)	271 (0.30)	176 (1.13)	272 (1.20)
40	153 (0.12)	270 (0.21)	156 (0.21)	277 (0.30)	183 (1.13)	269 (1.20)
50	165 (0.13)	286 (0.22)	171 (0.22)	275 (0.30)	189 (1.14)	274 (1.20)
60	197 (0.15)	298 (0.23)	200 (0.25)	281 (0.30)	196 (1.14)	296 (1.21)

[a] Numbers in parentheses indicate the effective Na^+ concentration (excess Na concentration + 0.24% of the DNA phosphate concentration). The relative error of the C_i and C_a values is ~5%.

Table II
Effective Radii of DNA Molecules and DNA Volume Fractions in Concentrated DNA Solutions in 0.01, 0.1, and 1.0 M Na^+ Buffers

	0.01 M Na^+				0.1 M Na^+				1.0 M Na^+			
t, °C	r_i,[a] Å	ν_i[c]	r_a,[b] Å	ν_a[c]	r_i,[a] Å	ν_i[c]	r_a,[b] Å	ν_a[c]	r_i,[a] Å	ν_i[c]	r_a,[b] Å	ν_a[c]
20	21.3	0.58	15.7	0.62	20.6	0.56	15.0	0.59	16.9	0.48	15.0	0.59
40	18.7	0.52	15.1	0.60	18.5	0.52	14.8	0.59	16.0	0.46	15.1	0.60
60	15.0	0.43	14.0	0.57	14.8	0.43	14.6	0.58	15.1	0.43	14.1	0.57

[a] The values of r_i were calculated by comparing the values of C_i (the critical DNA concentration required for the anisotropic-phase formation) with ν from Flory's theory[12] for $\chi = 0$. [b] The values of r_a were calculated by comparing the values of C_a (the DNA concentration at which the last trace of the isotropic phase disappears) with ν' from Flory's theory[12] for $\chi = 0$. [c] The volume fractions ν_i and ν_a were calculated from the formula $\nu = \pi r^2 L N_{AV}/M$, where r is the effective radius, L the length of DNA molecule (500 Å), N_{AV} is Avogadro's number, and M is the molecular weight of DNA (97 020).

buffer. As can be seen from Table II, the DNA volume fractions corresponding to the isotropic and anisotropic boundaries are comparable to the values calculated from Flory's theory for the values of axial ratio x ($x = L/D_{eff}$, where L is the length of DNA molecule and D_{eff} is its effective diameter) in the range of 11.9 (20 °C, 0.01 M Na^+) and 17.7 (60 °C, 1.0 M Na^+). For example, at 20 °C in 0.01 M Na^+ $\nu_a/\nu_i = 1.07$, and the value calculated from Flory's theory is 1.04. However, in our case the DNA molecules change their effective axial ratio as they approach the anisotropic boundary (their effective diameter decreases). If the DNA effective radius remained unchanged with increasing DNA concentration, then at 20 °C in 0.01 and 0.1 M Na^+ buffers the volume fraction of DNA molecules in solution would exceed unity before the anisotropy boundary was reached. Therefore, it seems inevitable that the effective DNA radius has to decrease with increasing DNA concentration. For the 1.0 M Na^+ buffer the DNA volume fraction at the anisotropic boundary would remain below unity if the effective radius of DNA would remain the same as at the isotropic boundary; hence it is possible that the effective DNA radius does not change with increasing DNA concentration in 1.0 M Na^+ buffer. On the other hand, DNA solutions with concentrations up to ~400 mg/mL in 0.1 M Na^+ buffer were prepared in our laboratory.[43] If the DNA effective radius remained at ~21 Å up to this concentration, the corresponding DNA volume fraction in solution would be ~1.6; therefore, the effective DNA radius has to decrease with increasing DNA concentration, at least up to 0.1 M Na^+.

Comparison with the Theory of Stroobants et al.[39] This theory is an extension of the Onsager[10] theory to the case of charged polymers and includes the effect of the electrostatic interaction between closely spaced polyelectrolyte molecules on the anisotropic-phase formation. In general, the most favorable arrangement of two charged rods that minimizes their electrostatic interaction is with their axes perpendicular to each other. However, such a configuration is not possible in concentrated solution; therefore the electrostatic energy minimization will manifest itself in a twisting effect, which will increase the critical polyelectrolyte concentration required for phase separation. The details of phase boundaries and DNA effective radii calculations according to this theory were given earlier.[29,30] Table III lists the DNA effective radii and theoretical phase diagram boundaries for 0.01, 0.1, and 1.0 M Na^+ buffers, respectively. Since r_{eff}, $C_{i,t}$, and $C_{a,t}$ do not change much with temperature, we have listed only their values at 20 and 60 °C at each ionic strength.

Table III
DNA Effective Radii and Phase Boundaries in 0.01, 0.1, and 1.0 M Na^+ Buffers Calculated According to Stroobants et al.[39]

Na^+ buffer, M	t, °C	r_{eff}, Å	$C_{i,t}$[a]	$C_{a,t}$[a]	$C_{i,t}$,[b] mg/mL	$C_{a,t}$,[b] mg/mL
0.01	20	25.6	3.669	4.718	58.9	75.8
	60	22.7	3.643	4.681	65.9	84.7
0.1	20	21.9	3.634	4.668	68.2	87.8
	60	21.1	3.624	4.655	70.5	90.5
1.0	20	15.2	3.511	4.497	94.9	121.6
	60	15.0	3.505	4.490	95.5	122.4

[a] Theoretical reduced concentrations calculated according to eqs 13 and 14.[30] [b] Theoretical reduced concentrations converted to milligrams per milliliter by using the effective diameters from the second column.

The temperature and ionic strength dependence trends are similar to those observed, but the calculated phase diagram boundaries are much lower than the experimental ones. However, the ratio of the experimental to theoretical values (i.e., C_i^{exp}/C_i^{theory}) improves with increasing Na concentration. The values of DNA effective radii, r_{eff}, are higher than the values obtained from the fit to Flory's theory for the isotropic boundary. Only in 0.01 M Na^+ buffer are the effective DNA radius and phase boundaries temperature dependent, although only slightly, and there is no temperature dependence of these quantities calculated for the 0.1 and 1.0 M Na^+ buffers.

Discussion

Anisotropic Phases Formed in Concentrated DNA Solutions. Two types of anisotropic phases were observed in concentrated DNA solutions at all three ionic strengths: the weakly birefringent (precholesteric) phase and the cholesteric phase. The precholesteric phase appeared first in solution, and then small areas of a cholesteric phase

developed within it with increasing DNA concentration. The weakly birefringent phase consisted of large areas of alternating dark and white bands. Livolant[21] reported a phase that she called "precholesteric", but its microscopic textures were different from the textures observed in our precholesteric phase. Polarized light microscopy and laser diffraction experiments showed that this phase could be a cholesteric phase with a very large pitch, varying from 10 to ≥50 μm.

The process of cholesteric-phase formation was similar at all three Na concentrations. As the DNA concentration increased, small areas of cholesteric phase appeared within the precholesteric phase and kept growing. The cholesteric-phase pitch was found to be ~2.1 μm and was independent of DNA concentration.[43] A value of ~2.5 μm was reported by Brandes and Kearns[18] for DNA solution in 60 mM NaCl at ~250 mg/mL DNA. The pitch of the cholesteric phase observed by Livolant[4] in a controlled drying experiment with high molecular weight DNA was 1.2 μm, whereas the pitch determined from the cholesteric organization of DNA molecules in dinoflagellate chromosomes in the same study was ~0.254 μm. The cholesteric pitch of equine sperm chromatin was found to be 0.176 μm.[1] The dependence of the cholesteric pitch on DNA length has not been determined in vitro, so the reason why the cholesteric pitch of the in vivo systems is so much smaller is not known.

In addition to these two phases another anisotropic phase was observed in 0.01 M Na^+ buffer solutions with DNA concentrations exceeding 204 mg/mL. The microscopic textures exhibited by this phase resembled some of the textures observed in smectic phases of small-molecule liquid crystals.[32] However, Livolant has shown recently[24] that DNA solutions with concentrations exceeding 300 mg/mL have columnar longitudinal order and hexagonal lateral order. The spacing between DNA helices were estimated to range from 28 to 40 Å.

Formation of the columnar phase from the cholesteric phase upon increase in DNA concentration would require an increase in the cholesteric pitch as the cholesteric superhelix unwound. Indeed, such unwinding was observed in DNA samples with concentrations exceeding 300 mg/mL, where the cholesteric pitch increased with increasing DNA concentration from ~2 to ~4.5 μm.[43]

In conclusion, we can present the following generalized scenario for the formation of liquid-crystalline phases in concentrated DNA solutions: The first anisotropic phase to appear is a cholesteric phase with a very large pitch (10–50 μm). With increasing DNA concentration small areas of a cholesteric phase are formed. As the number density of DNA molecules increases further, the cholesteric phase slowly changes into a columnar phase by a process involving unwinding of the cholesteric superhelices. At even higher DNA concentration the columnar phase would persist with DNA interhelical spacings decreasing with increasing DNA concentration.

Even though the critical DNA concentrations required for the anisotropic-phase formation are not very strongly dependent on the excess Na^+ concentration, formation of the columnar phase is. In 0.01 M Na^+ buffer the transitional phase (unwinding cholesteric) first appeared at 204 mg/mL (effective Na^+ concentration of ~0.16 M), whereas in 0.1 M Na^+ buffer unwinding could be observed only above 300 mg/mL[43] (effective Na^+ concentration of 0.32 M). Clearly, helix–helix interactions, especially electrostatic effects, must play a role in the formation of a specific molecular order.

Phase Diagrams and the Effective Radius of DNA. The problem of anisotropic-phase formation in polyelectrolyte solutions is closely related to the problem of counterion–polyelectrolyte interactions. As first predicted by Onsager,[10] solutions of rodlike molecules should separate into anisotropic and isotropic phases when a critical concentration of rods in solution is reached. If the rodlike molecules are charged, the electrostatic interactions will affect the anisotropic-phase formation in two ways. First, the electrostatic repulsion will result in an increase of the effective diameter of the rods, increasing the rods' effective volume and causing a decrease in the critical rod concentration required for the phase separation. Second, requirement for the electrostatic energy minimization will cause twisting of the rods with respect to each other, increasing the polymer concentration necessary for the anisotropic-phase formation. The effect of electrostatic interactions can be taken into account by treating the polyelectrolyte molecules as scaled particles, with their effective radii dependent on the solution's ionic strength. In general, the effective DNA radius is predicted to decrease with increasing ionic strength (in dilute solutions); therefore, if this remains true for the concentrated solutions, the critical DNA concentration required for the formation of the anisotropic phase should increase with increasing ionic strength.

The phase diagrams obtained by us at three supporting electrolyte concentrations are in good qualitative agreement with the predictions of Flory's theory. Moreover, the modest ionic strength dependence of the phase boundaries indicates that the critical DNA concentration required for the anisotropic-phase formation depends on the *effective* free Na^+ concentration. The qualitative agreement with the theory of Stroobants et al.[39] is also good, but the DNA concentrations at both phase boundaries are ~50% lower than the experimental values. One of the reasons for this discrepancy may be the fact that Onsager[10] theory, on which the considerations of Stroobants et al.[39] are based, does not take into account end effects and virial coefficients higher than second order.

Odijk[44] estimated the changes in the concentration of phase boundaries in solutions of short polymers due to the third virial coefficient and found that the effect was small. This conclusion is valid for axial ratios between 20 and 50. In our case the calculated axial ratios of DNA molecules range from 10 (in 0.01 M Na^+ buffer) to 17 (in 1.0 M Na^+ buffer) at 20 °C. For example, in 1.0 M Na^+ buffer at 20 °C the phase boundaries would shift by $\delta C_i = -1.3$ (see eq III.14 in ref 44), which is equivalent to (−35 mg/mL (scaling is the same as in the theory of Stroobants et al.[39]), and $\delta C_a = -1.2$, equivalent to −32 mg/mL; i.e., both the isotropic- and anisotropic-phase boundaries would be lower than those calculated from Stroobants' theory (see Table III).

Another possibility we should consider is the semiflexibility of even such short DNA fragments, which would cause an increase in the concentrations of phase boundaries and a narrowing of the biphasic region. The Onsager theory was extended to wormlike polyelectrolytes by Odijk.[44] The scaled polymer concentrations at the isotropic and anisotropic boundaries are $C_i = 5.409 + 4.72h$ and $C_a = 6.197 + 4.97h$, where h is the twisting parameter (as defined in ref 39). Using the value of $h = 0.153$ and $r_{eff} = 25.6$ Å (0.01 M Na^+ buffer at 20 °C; see Table III), we obtain the scaled phase boundary concentrations $C_i = 6.13$ and $C_a = 6.96$, corresponding to the DNA concentrations of ~98 and 112 mg/mL, at the isotropic and anisotropic boundaries, respectively. The value of C_i is still

lower than the experimental one (131 mg/mL), but is ~40 mg/mL higher than the value obtained from the theory of Stroobants et al.[39] Therefore, even though our DNA fragments are short, including the flexibility effect improves the agreement with experimental data. Recently Sato et al.[45] determined the phase equilibria for the solutions of xanthan, a weak polyelectrolyte, in varying NaCl concentrations. They found a very good agreement between their experimentally determined phase boundaries and the theoretical values calculated from the theory of wormlike polyelectrolytes.[44] However, xanthan has much lower linear charge density than DNA (1/30 Å^{-1} as compared at 1/1.7 Å^{-1}) and the molecules had a ratio L/P = 2.6 (where L is the length of the molecule and P the persistence length); therefore, one would expect a much better agreement with theory.

It is also interesting to examine how our experimental results agree with the predictions of the Khokhlov-Semenov theory,[46,47] which describes the liquid-crystalline-phase formation in solutions of semiflexible, neutral polymers. We shall use the formulas for the concentrations of phase boundaries as presented by Odijk[44] (eq IX.7). The persistence length of DNA is approximately 500 Å at moderate ionic strengths; therefore in our case L/P = 1. The scaled phase boundary concentrations (scaling is the same as in ref 39 since L/P = 1) are C_i = 8.426 and C_a = 8.686, which correspond to DNA concentrations of C_i = 135 mg/mL and C_a = 139 mg/mL for r_{eff} = 25.6 Å (0.01 M Na^+ buffer at 20 °C; see Table III). The experimentally determined isotropic boundary at this ionic strength and temperature is 131 mg/mL, in remarkable agreement with the theoretical value. However, one should be cautious not to draw a conclusion that semiflexibility alone can account for the phase behavior of our samples. At 1.0 M Na^+ buffer the isotropic-phase boundary is higher than predicted by ~40 mg/mL, which cannot be explained by the change in flexibility (i.e., the persistence length) alone. In conclusion, a third virial coefficient and end and flexibility effects should all be included in the theory describing phase transitions in solutions of short polyelectrolytes.

The experimental phase boundaries in concentrated DNA solutions were also determined in a sedimentation equilibrium experiment[31] at several ionic strengths. The critical DNA concentrations required for the isotropic-phase–anisotropic-phase transition were found to be 102 mg/mL in 0.2 M NaCl and 152 mg/mL in 1.0 M NaCl. These values are lower than the critical DNA concentrations determined by us for the same effective Na concentrations (136 mg/mL in 0.1 M Na^+ buffer and 171 mg/mL in 1.0 M Na^+ buffer, Table I) and are consistent with the fact that Brian et al.[31] used longer DNA molecules (average length of ~200 bp).

Theoretical predictions of the effective DNA radius in dilute DNA solutions can be divided into two categories. The first involves estimates of the effective DNA radii based on the calculations of the second virial coefficient of charged molecules in solution. Stigter[48] calculated the effective DNA diameters at various ionic strengths using the McMillan–Mayer solution theory and the Debye–Hückel form of the electrostatic potential around the DNA molecules. This approximation was justified by the consideration of the overlap of electric double layers far from DNA molecules. The effective diameter, D_{eff}, can be viewed as the distance between charged cylinders for which the repulsive electrostatic energy is ~0.5 kT. The second type of theoretical predictions concerns the Manning's radius, R_M.

Manning's counterion condensation (CC) theory[49] postulates that if the charge separation (A) on the polyelectrolyte is less than a Bjerrum length Q, given by

$$Q = e^2/\epsilon kT$$

(where e is the elementary charge, ϵ is the electric permittivity of the solvent, k is the Boltzmann constant, and T is the temperature), then a sufficient number of counterions will "condense" on the polyion to lower its charge density parameter

$$\zeta = Q/A$$

to unity. The fraction of condensed counterions is $1 - 1/\xi$. For DNA, A = 1.7 Å and Q = 7.12 Å at 20 °C, therefore ξ = 4.2 and the fraction of condensed ions is 0.76. The distance from the polyelectrolyte within which the condensed ions are found (Manning's radius, R_M) was predicted to be dependent only on the polymer charge density ξ.[50]

The Poisson–Boltzmann (PB) theory, hypernetted chain (HNC) theory, and Monte Carlo simulations have been used to estimate R_M's at different ionic strengths. LeBret and Zimm[51] showed that counterion condensation can be derived from the PB equation. They found that a constant fraction of condensed counterions remained within a finite distance from the polyelectrolyte even at infinite dilution. The distance containing the Manning's fraction of condensed counterions was proportional to $\kappa^{-1/2}$, where κ is the Debye screening parameter.

The HNC theory, which, unlike the PB theory, includes the short-range interactions between small ions and positional correlations between them, was used to calculate the R_M values for DNA in 0.001, 0.01, and 0.1 M monovalent salt.[52] At all salt concentrations the R_M values were larger than values obtained from the counterion condensation theory.[49] In an extension of this work[53] the values of R_M obtained for 0.01 and 0.001 M NaCl and a mixture of 0.14 M NaCl and 0.02 M $MgCl_2$ were compared with the results obtained from the PB theory and Monte Carlo simulations. It was found that the PB theory underestimates the counterion concentration within the Manning's radius by ~15% compared with the HNC and MC predictions.

Jayaram et al.[54] calculated the values of Manning's radius using the nonlinear Poisson–Boltzmann equation. These calculations included the detailed charge distribution of DNA molecules and assumed different polarizabilities of the macromolecule and the solvent.

The values of the DNA effective radii at several ionic strengths were determined experimentally by Brian et al.[31] for concentrated DNA solutions in a sedimentation equilibrium experiment. Nicolai and Mandel[55] determined the second virial coefficient (A_2) of 150-bp DNA fragments in solutions with DNA concentrations up to 35 mg/mL and NaCl concentrations from 0.002 to 0.5 M NaCl. The effective DNA radii were estimated from the values of A_2. Table IV lists the experimental values of r_{eff} obtained in refs 31 and 55 and the best-fit effective radii obtained by us. For comparison we have also included the theoretical values of r_{eff} and R_M calculated for dilute DNA solutions, as well as values of r_{eff} calculated from the theory of Stroobants et al.[39] for our concentrated DNA solutions.

All of the theoretical values in Table IV were calculated by using DNA molecules modeled as infinitely long cylinders of uniform charge density, without including any structural features of a DNA helix (with the exception of ref 54). It should be noted that there is no direct relationship between the values of r_{eff} and R_M. From Figure 2 in ref 54 it can be estimated that at a distance of 15.5

Table IV
Ionic Strength Dependence of the DNA Effective Radius (r_{eff}) and the Manning's Radius (R_M) at 20 °C

ref	salt concn, M 0.01	0.10	0.15	0.20	1.0
	r_{eff} (exptl), Å				
Brian et al.[31]				21.0	13.0
this paper[a]		21.3 (0.01)		20.6 (0.10)	16.9 (1.0)
Nicolai & Mandel[55]	66.0	21.5			
	r_{eff}(theor), Å				
Stroobants et al.[39b]			25.6 (0.01)	21.9 (0.10)	15.2 (1.0)
Stigter[48]	78.5	28.0		22.0	14.8
	R_M(theor), Å				
Manning[49]	14.6	14.4			12.6
LeBret & Zimm[51]	38.1	16.3			12.1
Bacquet & Rossky[52]	27.4	19.8			
Murthy et al.[53]	27.1		15.5		
Jayaram et al.[54]	19.5	15.4	15.4		12.9

[a] Numbers in parentheses indicate the excess Na^+ concentration. [b] Calculated for the three excess Na^+ concentrations given in parentheses.

Å from the DNA helix axis (equal to R_M at 0.15 M NaCl) the electrostatic potential is equal to ~1.5 kT, and it drops to 0.5 kT at ~21.5 Å, which is in very good agreement with the value of r_{eff} = 22 Å predicted by Stigter for 0.2 M NaCl, and with the experimental values of 21.5 Å in 0.1 M NaCl from ref 55, 21.3 Å (this work), and 21.0 Å in 0.2 M NaCl from ref 31. Therefore, it should be expected that the effective DNA radius will be larger than Manning's radius for a given ionic strength.

The comparison of the experimental values of r_{eff} shows very good agreement between our results and refs 31 and 55, except at 1.0 M Na^+. The theoretical prediction of Stigter[48] at 0.1 M NaCl (28 Å) is higher than the experimental values, but the 22-Å effective radius in 0.2 M NaCl agrees very well with the experimental results. It is also interesting that the value of 21.5 Å obtained from the determination of the second virial coefficient[55] at low DNA concentrations in 0.1 M NaCl is in excellent agreement with the value of 21.3 Å determined by us for the excess Na^+ concentration of 0.01 M (effective Na^+ concentration of 0.1 M).

Recently Podgornik et al.[56,57] presented results of osmotic pressure experiments on concentrated DNA solutions at different ionic strengths. The surface to surface separation between DNA molecules, measured by X-ray diffraction, ranged from 5 to 25 Å. The authors concluded that the observed force decay constants could not be explained by the results of Poisson–Boltzmann calculations and that another force (hydration force) had to be introduced. It is quite possible that at very small separations between DNA molecules in condensed solutions forces other than electrostatic could appear. These forces could result from microscopic electrostatic effects due to changes in counterion binding and distribution. In particular, our ^{23}Na NMR experiments[58] showed that the average electric field experienced by the counterions in the vicinity of DNA changes with DNA concentration and temperature in the liquid-crystalline phases. However, the question of whether such forces replace the electrostatic interactions totally cannot be answered until we have a clear picture of the short-range interactions between closely packed DNA helices.

Conclusions

Highly concentrated DNA solutions undergo a transition to the fully liquid crystalline state in accord with the theoretical predictions of Onsager[10] and Flory[11,12] and the observed behavior of uncharged, semirigid polymers. We have shown that this transition involves passage through a series of phases, regardless of the supporting electrolyte concentration. At the lowest DNA concentrations resulting in phase separation, the anisotropic phase is a poorly organized, slightly twisted nematic phase termed "precholesteric". Increasing the DNA concentration yields a well-defined cholesteric phase with a pitch of 2.1 μm. At very high DNA concentrations (>300 mg/mL) the cholesteric phase transforms into a columnar phase by gradual unwinding of the cholesteric superhelices.

The critical concentrations required for the appearance of anisotropic phase were only moderately sensitive to supporting electrolyte concentration, and the critical concentrations at which the isotropic phase disappeared were essentially insensitive to supporting electrolyte concentration. The limited influence of supporting electrolyte can be attributed in part to the high critical concentrations observed for these relatively short DNA fragments and the resulting large contribution of DNA counterions to the pool of free Na^+ ions. Low concentrations of supporting electrolyte primarily seem to increase the range of DNA concentrations over which pretransitional phenomena are observed (see also ref 30).

The critical concentrations for anisotropic-phase formation were in good agreement with the theory of Flory[11,12] when the effective radius was treated as a scaling factor. Best-fit radii calculated in this manner (from 22 to 17 Å) agreed well with other experimental and theoretical values of the effective DNA radii at the ionic strengths corresponding to the effective Na^+ concentrations in our solutions. Good agreement was also found with Onsager theory expanded to polyelectrolytes by Stroobants et al.,[39] provided effects of finite chain flexibilty were incorporated as described by Odijk[44] or Khokhlov and Semenov.[46,47] A recent study[45] on the ionic strength dependence of phase transitions for xanthan suggests that the latter approach should be used for moderately long polyelectrolytes. In this respect, the length dependencies of phase transitions of DNA, which is a much stronger polyelectrolyte, are of considerable interest.

Acknowledgment. We are grateful to Dr. Richard Rosanske and Dr. Tom Gedris for their assistance with NMR measurements and to Michael Waley from the University of Florida Training Reactor Facility in Gainsville for help with the nuclear activation analysis of DNA samples. This research was supported in part by NIH Grant GM 37098.

References and Notes

(1) Sipski, M. L.; Wagner, T. E. *Biopolymers* **1977**, *16*, 573.
(2) Livolant, F.; Bouligand, Y. *Chromosoma* **1978**, *68*, 21.
(3) Livolant, F.; Bouligand, Y. *Chromosoma* **1980**, *80*, 97.
(4) Livolant, F. *Eur. J. Cell Biol.* **1984**, *33*, 300.
(5) Rill, R. I.; Livolant, F.; Aldrich, H. C.; Davidson, M. W. *Chromosoma*, in press.
(6) Stroud, R. M.; Serwer, P.; Ross, M. J. *Biophys. J.* **1981**, *36*, 743.
(7) North, A. C. T.; Rich, A. *Nature* **1961**, *191*, 1242.
(8) Earnshaw, W. C.; Harrison, S. C. *Nature* **1977**, *268*, 598.
(9) Subirana, J. A.; Lloveras, J.; Lombardero, M.; Viñuela, E. *J. Mol. Biol.* **1979**, *128*, 101.
(10) Onsager, L. *Ann. N.Y. Acad. Sci.* **1949**, *51*, 627.
(11) Flory, P. J. *Proc. R. Soc. London* **1956**, *A234*, 60.
(12) Flory, P. J. *Proc. R. Soc. London* **1956**, *A234*, 73.
(13) Robinson, C. *Tetrahedron* **1961**, *13*, 219.
(14) Bouligand, Y.; Livolant, F. *J. Phys.* **1984**, *45*, 1899.
(15) Livolant, F. *J. Phys.* **1986**, *47*, 1605.
(16) Rill, R. L. *Proc. Natl. Acad. Sci. U.S.A.* **1986**, *83*, 342.
(17) Strzelecka, T. E.; Rill, R. L. *J. Am. Chem. Soc.* **1987**, *109*, 4513.
(18) Brandes, R.; Kearns, D. R. *Biochemistry* **1986**, *25*, 5890.

(19) Iizuka, E.; Kondo, Y. *Mol. Cryst. Liq. Cryst.* **1979**, *51*, 285.
(20) Iizuka, E. *Polym. J.* **1978**, *10*, 237.
(21) Livolant, F. *J. Phys.* **1987**, *48*, 1051.
(22) Strezelecka, T. E.; Davidson, M. W.; Rill, R. L. *Nature* **1988**, *331*, 457.
(23) Livolant, F.; Bouligand, Y. *J. Phys.* **1986**, *47*, 1813.
(24) Livolant, F. *Nature* **1989**, *339*, 724.
(25) Lerman, L. S. *Cold Spring Harbor Symp. Quant. Biol.* **1974**, *38*, 59.
(26) Maniatis, T.; Venable, J. H.; Lerman, L. S. *J. Mol. Biol.* **1974**, *84*, 37.
(27) Giannoni, G.; Padden, F. J., Jr.; Keith, H. D. *Proc. Natl. Acad. Sci. U.S.A.* **1969**, *62*, 964.
(28) Lerman, L. S.; Wilkerson, L. S.; Venable, J. H.; Robinson, B. H. *J. Mol. Biol.* **1976**, *108*, 271.
(29) Strzelecka, T. E. Ph.D. Dissertation, FSU, 1988.
(30) Strzelecka, T. E.; Rill, R. L. *Biopolymers* **1990**, *30*, 57.
(31) Brian, A. A.; Frisch, H. L.; Lerman, L. S. *Biopolymers* **1981**, *20*, 1305.
(32) Gary, G. W.; Goodby, J. W. G. In *Smectic Liquid Crystals*; Leonard Hill: Glasgow, 1984.
(33) Shindo, H.; Wooten, J. B.; Pheiffer, B. H.; Zimmerman, S. B. *Biochemistry* **1980**, *19*, 518.
(34) Nall, B. T.; Rothwell, W. P.; Waugh, J. S.; Rupprecht, A. *Biochemistry* **1981**, *20*, 1881.
(35) Di Verdi, J. A.; Opella, S. J. *J. Mol. Biol.* **1981**, *149*, 307.
(36) Doddrell, D.; Glushko, V.; Allerhand, A. *J. Chem. Phys.* **1972**, *56*, 3683.
(37) Hogan, M. E.; Jardetzky, O. *Biochemistry* **1980**, *19*, 3460.
(38) Bolton, P. H.; James, T. L. *J. Phys. Chem.* **1979**, *83*, 3359.
(39) Stroobants, A.; Lekkerkerker, H. N. W.; Odijk, T. *Macromolecules* **1986**, *19*, 2232.
(40) Flory, P. J.; Ronca, G. *Mol. Cryst. Liq. Cryst.* **1979**, *54*, 289.
(41) Flory, P. J.; Ronca, G. *Mol. Cryst. Liq. Cryst.* **1979**, *54*, 311.
(42) Warner, M.; Flory, P. J. *J. Chem. Phys.* **1980**, *73*, 6327.
(43) Van Winkle, D. H.; Davidson, M. W.; Chen, W.-X.; Rill, R. L. *Macromolecules* **1990**, *23*, 4140.
(44) Odijk, T. *Macromolecules* **1986**, *19*, 2313.
(45) Sato, T.; Kakihara, T.; Teramoto, A. *Polymer* **1990**, *31*, 824.
(46) Khokhlov, A. R.; Semenov, A. N. *Physica A (Amsterdam)* **1981**, *108*, 546.
(47) Khokhlov, A. R.; Semenov, A. N. *Physica A (Amsterdam)* **1982**, *112*, 605.
(48) Stigter, D. *Biopolymers* **1977**, *16*, 1435.
(49) Manning, G. S. *J. Chem. Phys.* **1969**, *51*, 924.
(50) Manning, G. S. *Biophys. Chem.* **1977**, *7*, 95.
(51) LeBret, M.; Zimm, B. H. *Biopolymers* **1984**, *23*, 287.
(52) Bacquet, R.; Rossky, P. J. *J. Phys. Chem.* **1984**, *88*, 2660.
(53) Murthy, C. S.; Bacquet, R.; Rossky, P. J. *J. Phys. Chem.* **1985**, *89*, 701.
(54) Jayaram, B.; Sharp, K. A.; Honig, B. *Biopolymers* **1989**, *28*, 975.
(55) Nicolai, T.; Mandel, M. *Macromolecules* **1989**, *22*, 438.
(56) Podgornik, R.; Rau, D. C.; Parsegian, V. A. *Macromolecules* **1989**, *22*, 1780.
(57) Podgornik, R.; Parsegian, V. A. *Macromolecules* **1990**, *23*, 2265.
(58) Strzelecka, T. E.; Rill, L. R. *Biopolymers* **1990**, *30*, 803.

Registry No. Na^+, 17341-25-2